JOURNAL OF AIRCRAFT
Vol. 38, No. 5, September–October 2001

Jet/Intake Interference in Short Take off, Vertical Landing Aircraft

A. J. Saddington* and K. Knowles†
Cranfield University, RMCS, Shrivenham, Wiltshire SN6 8LA, United Kingdom

An experimental programme was conducted to investigate the aerodynamic interference effects between the jet- and intake-induced flows and the lifting surfaces of a generic jet-lift short take-off and vertical landing aircraft in transitional flight, out of ground effect. The tests were carried out in an open-jet wind tunnel, and the model was equipped with a single, variable position, vectored lift-jet and powered intakes. Static pressure measurements were made on the wing and intake lips from which airloads were inferred. The effect of jet to intake mass flow ratio on jet/intake aerodynamic interactions was investigated. The experiments conclude that a mutual interference exists between the jet and intake flows, which generates nonlinearly additive loads on the airframe. The combined jet- and intake-induced interference on the wing increased with increasing jet to intake mass flow ratio. Ignoring jet/intake interference effects gave a consistently lower overall wing root lift loss, which was equivalent to up to 0.75 deg of incidence.

Nomenclature

A_i = throat area of one intake [0.002], m^2
C_l = sectional lift coefficient, $\{l/q_\infty c\}$
C_{ni} = intake normal force coefficient,

$$\left\{ \sum \frac{p_i - p_\infty}{q_\infty} \right\}$$

C_p = pressure coefficient $\{(p - p_\infty)/q_\infty\}$
c = wing chord, m
d_{ie} = equivalent intake diameter $\sqrt{(4A_i/\pi)}$
d_n = nozzle diameter [0.0254], m
l = sectional lift, N
M = Mach number
P = total pressure, Pa
p = static pressure, Pa
q = dynamic pressure, Pa
V = velocity, ms^{-1}
V_e = effective velocity ratio $\{(M_\infty/M_j)\sqrt{(p_\infty/p_j)}\}$
$\Delta C_{l(\text{root})}$ = $\{C_{l(\text{root})}/C_{l(\text{root})}(\text{datum})\} - 1$
ρ = density, kgm^{-3}

Subscripts

a = atmospheric (outside working section)
c = settling chamber
j = jet
root = wing root
∞ = freestream (crossflow)

Introduction

SHORT take off, vertical landing (STOVL) aircraft introduce many aerodynamic characteristics unique to their operation. The flow fields surrounding such aircraft during transition from hover to wingborne flight are of particular importance. Transitional flight is dominated by the phenomenon of the jet in cross-flow, which has, consequently, received considerable attention in the literature.[1] The jet in crossflow is, however, only one element of the flowfield surrounding a STOVL aircraft during transition. It is essential to determine the overall performance of STOVL designs during this critical flight regime and account for the interference effects between the airframe and the entire propulsion system.

During wind-tunnel testing of jet-lift STOVL aircraft, it is usual to simulate the jet efflux but not the intake flows. The intakes, which are commonly faired over or are unpowered, are generally tested in separate wind-tunnel experiments. This procedure, however, ignores any mutual interferences that might exist between jets, intakes, and wings, but is adopted because of the complexity and expense of building a fully powered, fully metric STOVL wind tunnel model. The forces acting on the wind tunnel model are deduced by the linear addition of the forces measured from the two separate tests. There is some doubt as to the validity of this approach, particularly for STOVL aircraft with their close-coupled lift systems.[2]

Some research has been done in the past in an attempt to ascertain the significance of jet/intake interference effects on a wind-tunnel model. These studies, however, have suffered from unrepresentatively low intake mass flow rates relative to the jets[3] or low Reynolds number and Mach number jet flows.[4] Other works[5,6] have only presented total forces and moments or surface pressures, and little attempt has been made to isolate and identify any possible jet/intake interference effects.

More recently, we have carried out an experiment at the Royal Military College of Science (RMCS) to measure jet/intake interference effects on a generic STOVL jet-lift aircraft under constant jet/intake mass flow ratio conditions.[7] Both jet and intake flows were simulated at realistic conditions, and measurements were made of wing and intake pressures from which airloads were inferred. The results concluded that a mutual jet/intake interference effect did indeed occur for the STOVL configuration tested confirming the concerns Harris et al.[2] had regarding the superposition of separate jet and intake force measurements. With both intakes powered and jet blowing, the resultant effect on the wing lift was not the numerical sum of the two in isolation.[7] Mutual interference effects were found to be generally insensitive to nozzle pressure ratio (NPR) $\{P_c/P_a\}$ at constant jet to intake mass flow ratio.[7] Nozzle position (forward of the intake plane) also had little influence on the interference effect.[7]

The work presented here extends that described earlier by examining the effect of varying jet to intake mass flow ratio on the jet/intake interference effects.

Received 5 August 2000; revision received 1 June 2001; accepted for publication 12 June 2001.

*Lecturer, Aeromechanical Systems Group, Department of Aerospace, Power and Sensors.
†Head, Aeromechanical Systems Group, Department of Aerospace, Power and Sensors. Senior Member AIAA.

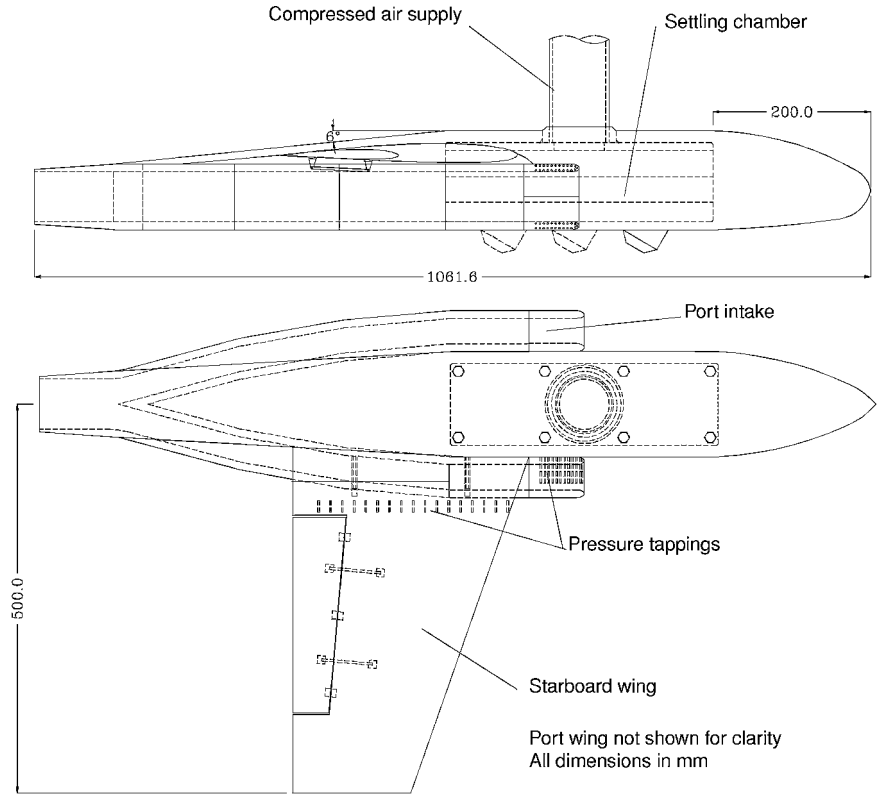

Fig. 1 Schematic layout of the wind-tunnel model.

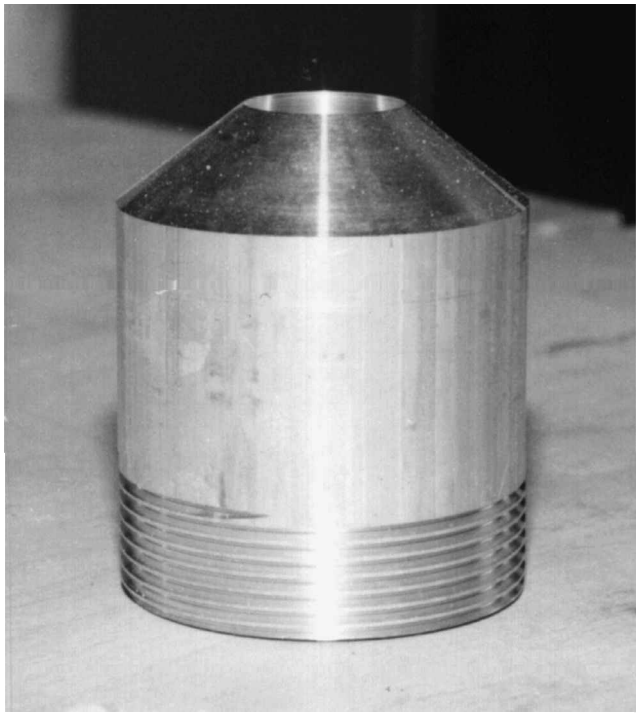

Fig. 2 Jet nozzle used in the tests.

Wind-Tunnel Model

To maintain consistency with previous work, the same wind-tunnel model was used for these experiments (Fig. 1). It was a tailless generic STOVL aircraft with a shoulder-mounted wing of approximately 1-m span and rectangular side-mounted intakes.

Jet Simulation

A single convergent jet nozzle (Fig. 2) of 25.4 mm exit diameter was provided, representing the forward lift jet, vectored aft 60 deg to the horizontal. The nozzle was of a simple convergent design.[8] The nozzle convergence had a length equal to one-quarter of the exit diameter and a half angle of 10 deg. The nozzle could be located in one of three different positions relative to the wing and intakes: 90 mm aft of the intake plane (approximately in line with the wing root leading edge), in the same plane as the intake, or 90 mm ahead of the intake plane. The jet was powered by compressed air at ambient temperature and fed to the nozzle via a settling chamber situated in the fuselage (Fig. 1). Nozzle mass flow rate was varied by changing the NPR.

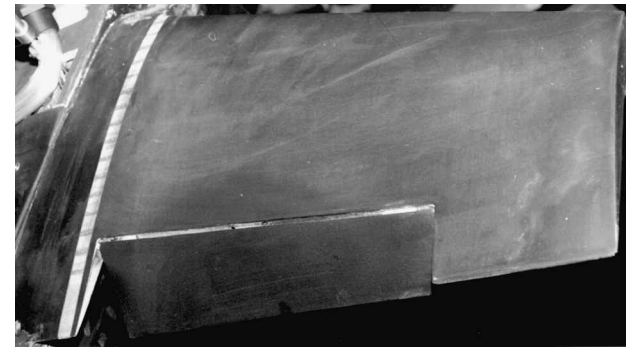

Fig. 3 Starboard wing showing the flap and pressure tappings.

Wing

The wing had a NACA 1408 section with a moderately swept and tapered planform (Fig. 3). A plain flap was included with a hinge line at 75% chord. The flap extended from 30 to 70% semispan and could be deflected up to 50 deg. For these tests, a flap setting of 45 deg was used. A total of 33 static pressure tappings, at spacings of approximately 5% chord, were set into the starboard wing upper and lower surfaces at 25% semispan. The pressure tappings were 0.5 mm in diameter.

Intakes

The intakes were rectangular in section with a 2:1 aspect ratio and parallel sides. The lip section was elliptical with a 3:1 aspect ratio.

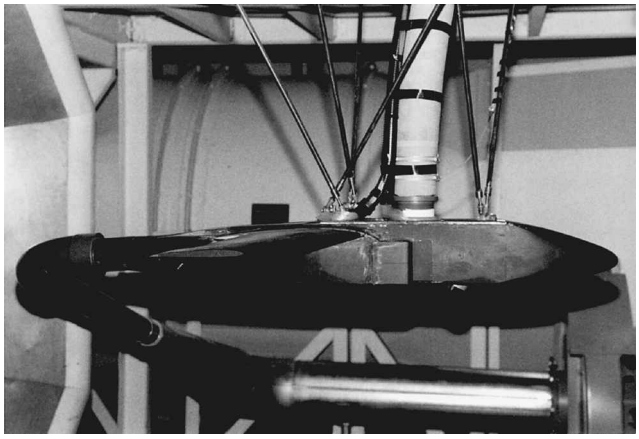

Fig. 4 Side view of the model in the RMCS 1.5 × 1.1 m open-jet wind tunnel.

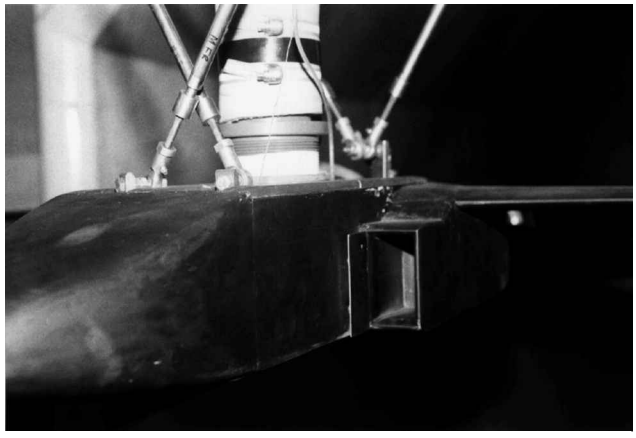

Fig. 5 Support struts and compressed air supply to the model.

The intakes were ducted along the sides of the fuselage and then combined to form a single circular exit at the rear of the model. A total of 46 static pressure tappings, of 0.5 mm diameter, were located on the starboard intake nacelle centerline, around the lip area, and extended aft to approximately one equivalent intake diameter d_{ie} on the inner and outer surfaces of the upper and lower intake walls. The intake airflow was provided by a large centrifugal fan connected to the model via 65-mm-diam duct work, which included two 90 deg bends and diffused to 225 mm diameter before the fan (Fig. 4).

Test Facilities

Tests were carried out in an open-jet wind tunnel at RMCS. The tunnel nozzle is elliptical with dimensions of 1.5 m wide by 1.1 m high, and the working section is 2 m long. Dynamic pressure was measured using a method suggested by Kuenstner et al.[9] The wind-tunnel control system was adapted so that the fan could be computer controlled by a 286-based personal computer. Working section dynamic pressure was held to a tolerance of ±0.25% using this system.

The model was located centrally in the working section and supported on five adjustable struts enabling pitch, roll, and yaw adjustment (Fig. 5). For the current tests no pitch, roll, or yaw angles were set, the wing being at 0 deg angle of attack. Note, however, that the wing was lifting due to the 1% wing camber and the 45 deg flap setting.

Compressed air was supplied to the fuselage settling chamber through a 63.5-mm-diam semi-flexible hose to the top of the model (Fig. 5). Two screw-type Howden compressors were available to supply up to 0.9 kgs^{-1} at 7 bar gauge, running in series, or 1.8 kgs^{-1} at 4 bar gauge, running in parallel. This permitted tests to be run continuously. NPR was also computer controlled to a tolerance of ±0.25% using the same system that controlled the wind tunnel but running on a separate 486-based personal computer.

Table 1 Mass flows and ratios for the tests

NPR	Jet $\dot{m}$, kgs^{-1}	Mass flow ratio
1.0	N/A	0.0
1.586	0.189	0.440
2.0	0.244	0.567
3.0	0.367	0.853
4.0	0.489	1.137

Experimental Procedure

The compressor driving the intake suction was not speed controlled and so the intake mass flow rate was held constant at 0.43 kgs^{-1}. The total intake area $2A_i$ was 0.004 m^2, which gave a mean intake throat Mach number of approximately 0.3. For a nominal intake Mach number of 0.3, the capture area ratio A_∞/A_i was 10.2, 5.1, and 3.4 at crossflow velocities of 10, 20, and 30 ms^{-1}, respectively. The jet mass flow rate was varied by changing the NPR. Theoretical jet mass flow rates and jet/intake mass flow ratios are given in Table 1.

Tests were carried out under the following conditions:

1) NPRs of 1.586, 2.0, 3.0, and 4.0;

2) three different nozzle positions (forward, center and rearward);

3) crossflow velocities of 10, 20, and 30 ms^{-1} (nominal velocity); and

4) out of ground effect (the model was 1.5 m, or approximately 60 nozzle diameters, from the laboratory floor).

Four model configurations were tested:

configuration A, intakes faired, jet off;

configuration B, intakes faired, jet on;

configuration C, intakes powered, jet off; and

configuration D, intakes powered, jet on.

When the jet was off, the nozzle was replaced by a blank, leaving the lower surface of the fuselage flush. By comparison, the nozzle protruded slightly below the fuselage, as can be seen from Figs. 1 and 4.

Results and Discussion

Results are categorized as follows.

1) Configuration A provided the datum wing pressure distribution case.

2) Configuration B, when compared with configuration A, shows the effect of the jet flowfield on the wing C_p distribution.

3) Configuration C, when compared with configuration A, shows the effect of the intake flowfield on the wing C_p distribution.

4) Configuration D, when compared with configuration A, shows the simultaneous effect of the jet and intake flows on the wing C_p distribution.

Finally, the important comparison will be made between the two methods of determining the total interference effect of the jet and intakes on the wing: 1) the linear addition of configuration B and C results and 2) the configuration D results.

To enable the calculation of $C_{l(\text{root})}$, a C_p value of 0.0 at $x/\text{chord} = 1.0$ was added to the recorded data. Although this figure may be incorrect, its inclusion permits comparisons to be made. The parametric effects observed were considered more important at this stage than the exact numerical values. The measured wing root static pressures were integrated along the chord to give the sectional lift coefficient $C_{l(\text{root})}$. Only linear variations between data points were used for this integration. Although this undoubtedly leads to some errors, particularly in the leading-edge region, they were not felt to be significant for comparative purposes.

Fluctuations in wind-tunnel dynamic pressure have a direct influence on the measured static pressures on the model. The tolerance on the wind tunnel control software was set to ±0.25%. The manufacturer's quoted error for the pressure transducer measuring the static pressures is 1% of reading. Errors due to temperature drift and fluctuations in NPR were estimated to account for a further 0.25% error in the static pressure readings. Jet operation was found to have no measurable effect on model incidence, which was attributed to the rigid support structure. The theoretical error in static pressure

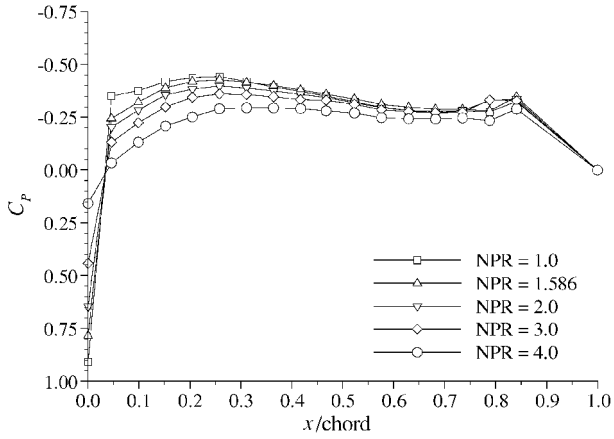

Fig. 6 Wing upper surface pressure distribution, intakes faired, forward nozzle position, q_∞ = 61.3 Pa.

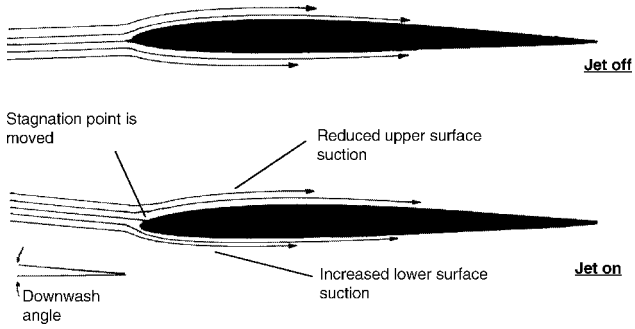

Fig. 7 Main jet-induced interference effects on the wing.

measurement was, therefore, taken to be ±1.5%. When integrated, the C_p distributions would also contain an error of ±1.5%. The combination of C_p distributions to obtain force coefficients would compound this error to ±3% for $C_{l(\text{root})}$ and ±6% for C_{ni}. The estimated errors are shown as vertical bars in the appropriate graphs. This does not include additional, unquantified errors due to the spatial resolution of the pressure tappings as discussed earlier.

Effect of the Jet on the Wing

Figure 6 shows a typical wing upper surface pressure distribution for the five different NPRs at a freestream velocity of 10 ms^{-1}. The effect of the jet was to reduce the suction pressures on the forward section of the wing up to about the 50% chord point, although for an NPR of 4.0, the wing pressure distribution was changed all of the way back to the rearmost pressure tapping. There were also relatively large changes in the leading-edge static pressures, indicating a significant shift in the forward stagnation point. The observed jet-induced interference effect was due to the vertical component of the jet entrainment flowfield (Fig. 7).

From the graph it is clear that as nozzle mass flow rate was increased the jet-induced interference on the pressure distribution increased also. This was attributed to the stronger downwash generated as the mass flow rate of the jet was increased. A computational fluid dynamics (CFD) simulation was developed to provide additional insight into the downwash flowfield generated by the jet. The simulation consisted of a simple round turbulent jet inclined at 30 deg to a flat plate, simulating the conditions on the underside of the wind-tunnel model. A Reynolds-averaged Navier–Stokes code (the commercial PHOENICS code) employing the k–ε turbulence model was run with a structured hexahedral mesh of approximately 125,000 cells. The CFD simulation showed that there was a distinct difference in the downwash velocity (Fig. 8) at different nozzle mass flow rates up to a freestream distance of about $10d_n$ (Ref. 10).

On the lower surface of the wing (Fig. 9) there was the usual jet-induced suckdown effect present. The effect of varying nozzle mass flow rate can also be seen in Fig. 9. Increasing mass flow rate increased the suction pressures forward of the 75% chord point reducing the overall lift on the wing. As with the upper surface, the

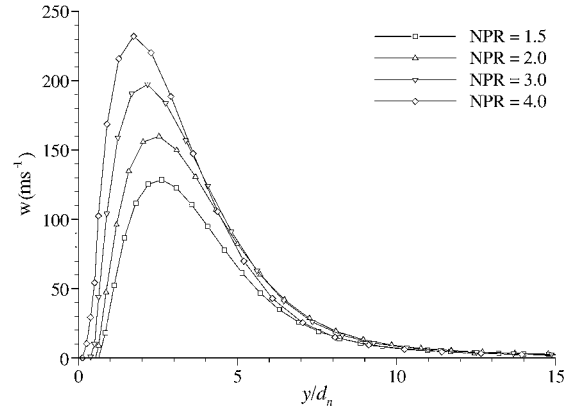

Fig. 8 CFD-predicted downwash for a round jet vectored 60 deg, $5d_n$ below nozzle exit, q_∞ = 61.3 Pa.

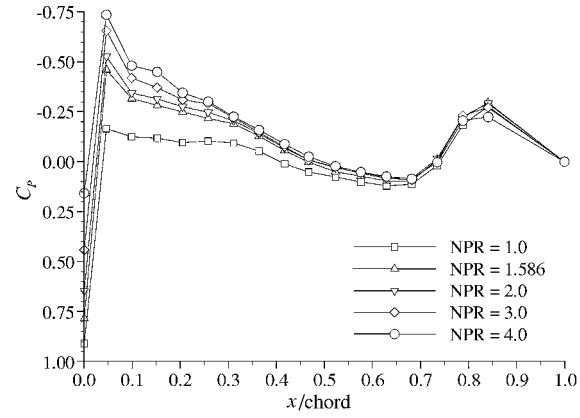

Fig. 9 Wing lower surface pressure distribution, intakes faired, forward nozzle position, q_∞ = 61.3 Pa.

higher the mass flow rate, the greater the jet-induced interference. Upper and lower surface pressure distributions were integrated to give the wing root sectional lift coefficient $C_{l(\text{root})}$. The jet-induced lift loss was given by the difference of the jet off (configuration A) and jet on cases (configuration B).

In all cases, the jet operation was detrimental to the aerodynamic performance of the wing and resulted in wing root sectional lift losses $\Delta C_{l(\text{root})}$ of between −0.042 (−17.5%) and −0.234 (−89.4%). The three-dimensional lift curve slope for the wing was calculated to be 3.764/rad (Ref. 11). The observed change in $C_{l(\text{root})}$ was equivalent, therefore, to a reduction in wing root incidence of between 0.6 and 3.6 deg. This agrees quite well with Mineck and Margason's[5] aircraft for which jet-induced lift loss resulted in a reduction in wing incidence of 0.4 deg at $V_e = 0.1$.

Increasing nozzle mass flow rate increased the jet-induced interference effect on the wing. Effective velocity ratio also had a strong influence on the jet-induced interference. The lower V_e is, the greater the interference. Nozzle position, however, did not have a strong influence on the interference effect. Table 2 summarizes the effect of the jet on $C_{l(\text{root})}$ for the center nozzle position.

Effect of the Intake on the Wing

Figure 10 shows the wing upper surface pressure distribution with the intakes faired and with the intakes powered for 10-ms^{-1} crossflow velocity. The intake flow reduced the suction pressures on the upper surface of the wing, forward of the 50% chord point. The overall effect was that the wing upper surface lift was reduced. The reason for the change was the presence of the intake flow. With the intakes faired, the airflow over the upper surface of the wing was relatively unobstructed by any part of the airframe.

With the intakes powered, however, the intake capture streamtube deflected the flow ahead of the wing, which changed the local flow direction of the freestream air flowing over the wing upper surface. This resulted in the observed changes (Fig. 11).

Table 2 Effect of the jet on $C_{l(\text{root})}$ (center nozzle position)

NPR	V_e	$C_{l(\text{root})}$	$\Delta C_{l(\text{root})}$
1.0	∞	0.261	N/A
1.586	0.035	0.185	−0.077
2.0	0.029	0.148	−0.113
3.0	0.023	0.096	−0.165
4.0	0.020	0.045	−0.216
1.586	0.070	0.194	−0.061
2.0	0.057	0.175	−0.079
3.0	0.047	0.176	−0.078
4.0	0.040	0.174	−0.080
1.586	0.105	0.198	−0.043
2.0	0.086	0.182	−0.059
3.0	0.070	0.171	−0.070
4.0	0.061	0.159	−0.082

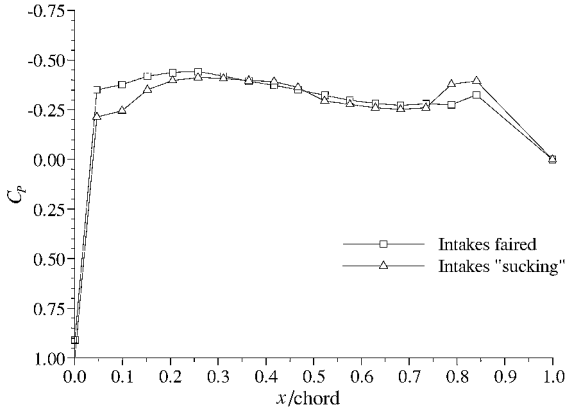

Fig. 10 Wing upper surface pressure distribution, jet off, q_∞ = 61.3 Pa.

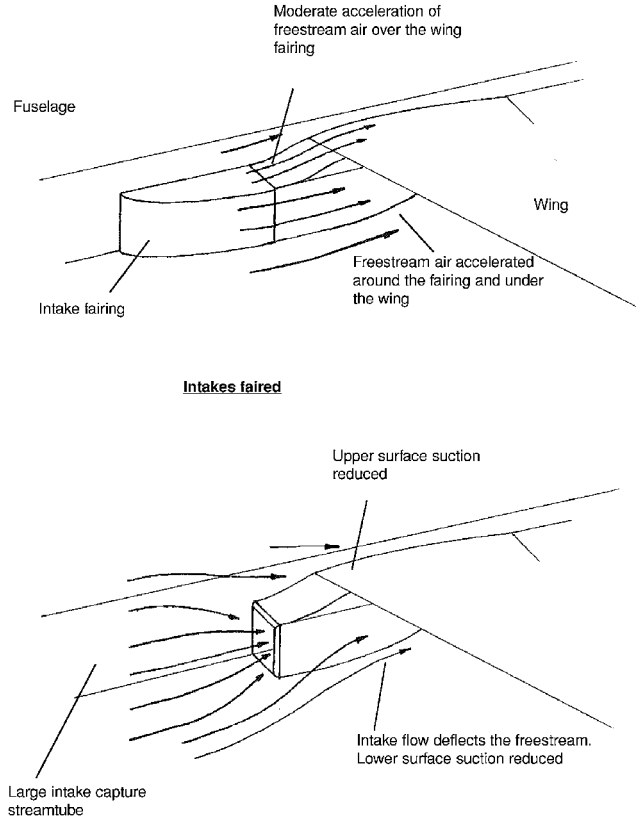

Fig. 11 Observed intake/wing interference effects.

Table 3 Effect of the intake on the wing

q_∞, Pa (V_∞, ms^{-1})	Intakes powered	$C_{l(\text{root})}$	$\Delta C_{l(\text{root})}$
61.3 (10)	No	0.261	N/A
61.3 (10)	Yes	0.317	0.056
245 (20)	No	0.254	N/A
245 (20)	Yes	0.277	0.022
511 (30)	No	0.241	N/A
511 (30)	Yes	0.251	0.010

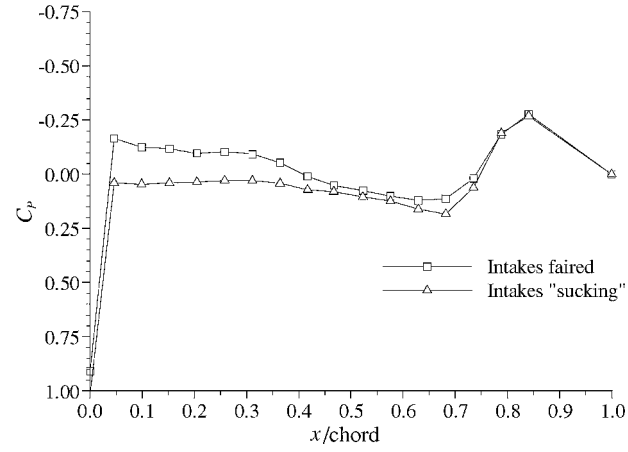

Fig. 12 Wing lower surface pressure distribution, jet off, q_∞ = 61.3 Pa.

Visualization of the flow around the intake and wing leading edge, using a tuft probe, indicated that the intake introduced a downward velocity component into the freestream ahead of and above the wing leading edge. At a freestream dynamic pressure of 61.3 Pa (10-ms^{-1} nominal crossflow velocity), the capture area ratio of the intake was approximately 10, and so this effect was quite noticeable. As the freestream dynamic pressure was increased, the capture area ratio of the intake decreased, becoming 5 at 245 Pa (20-ms^{-1} nominal crossflow velocity) and 3 at 551 Pa (30-ms^{-1} nominal crossflow velocity). This resulted in a smaller change in flow direction into the intake. Hence, the intake-induced interference reduced with increasing dynamic pressure.

On the lower surface of the wing (Fig. 12), the effect of the intake flow was more marked than on the wing upper surface. With the intakes powered, the suction pressures over most of the lower surface of the wing were more positive, increasing the lift on the wing. With the intakes faired, the freestream air was accelerated by the fairing before passing under the wing lower surface.

With the fairing removed, this acceleration was no longer present. Most of the air that would be diverted around the intake and over the wing was now being sucked into it (Fig. 11). As a result, the air flowing under the wing was of a lower velocity. This is thought to be the main reason for the difference between the two cases. There will also be a capture streamtube deflection effect similar to that on the upper surface. As with the upper surface, increasing freestream dynamic pressure reduced the intake-induced interference effect. Integrating the upper and lower surface pressure distributions to obtain $C_{l(\text{root})}$ showed that with the intakes powered the upper surface lift contribution was reduced at all freestream dynamic pressures. The percentage reduction was highest at the lowest freestream dynamic pressure. On the lower surface, the intakes powered condition gave a lift enhancement that was greater than the reduction on the upper surface. The net effect was that the wing generated more aerodynamic lift with the intakes powered than with the intakes faired (Table 3).

At a freestream dynamic pressure of 61.3 Pa, the effective increase in wing incidence due to intake suction was approximately 0.5 deg, reducing to 0.2 deg at 245 Pa and 0.1 deg at 551 Pa. Mineck and Schwendemann[6] determined from force and moment data that the effect of intake plugs on their model was effectively to reduce the

angle of attack of the wing by 1–2 deg. When it is considered that the intakes on their model were proportionately larger than on the one presented here, the 0.5 deg increase in wing root incidence would seem reasonable. Note that both these experiments used a model with a high-mounted wing. A mid- or low-mounted wing would undoubtedly give different results.

Effect of the Jet on Intake Flow

To determine the extent to which the jet altered the intake flow, the pressure distributions around the intake lips were examined. In general, the jet entrainment introduced a localized velocity component into the freestream that deflected the intake capture streamtube (Fig. 13).

Figure 14 shows a typical intake lower outer surface pressure distribution for the center nozzle position. In this case the freestream dynamic pressure is 551 Pa. With the jet off, the C_p values on the majority of the lower outer surface of the intake were zero. This is typical of the pressure distribution on a flat surface at 0 deg incidence to the freestream. Nearer the intake lip, the static pressure increases until the stagnation point is reached which, although not clearly captured on the graph, is nevertheless on the outer surface of the intake. This indicates that even at the highest freestream dynamic pressure, the intake is operating at a high level of suction, consistent with a STOVL aircraft operating at high power levels and low forward speed.

With the jet blowing, the C_p values on the lower outer surface of the intake were substantially more negative than with the jet off, of

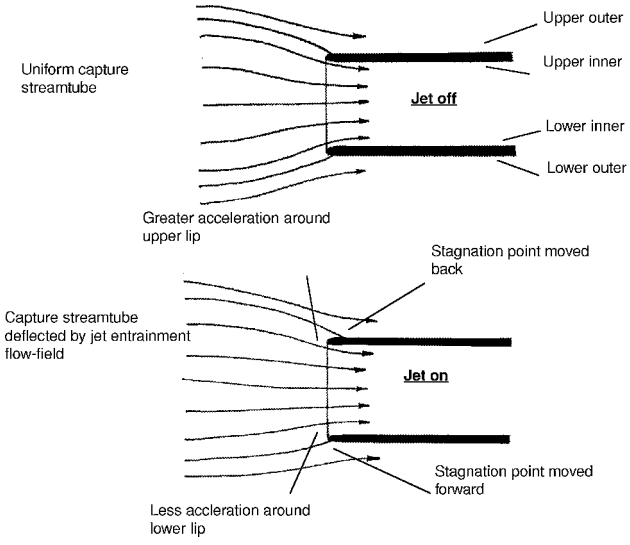

Fig. 13 Jet-induced interference effects on the intake.

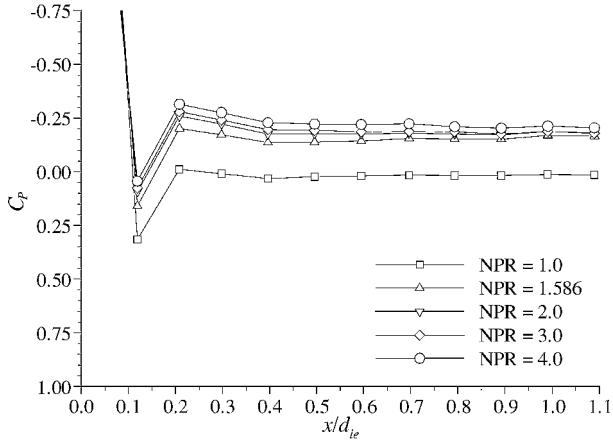

Fig. 14 Intake lower outer surface pressure distribution, intakes powered, center nozzle position, q_∞ = 551 Pa.

Table 4 Effect of the jet on the intakes, center nozzle position

NPR	V_e	C_{ni}	ΔC_{ni}
1.0	∞	−3.343	N/A
1.586	0.035	−4.472	−1.129
2.0	0.029	−4.922	−1.579
3.0	0.023	−5.837	−2.494
4.0	0.020	−6.215	−2.873
1.0	∞	−0.934	N/A
1.586	0.070	−1.402	−0.467
2.0	0.057	−1.508	−0.574
3.0	0.047	−1.619	−0.684
4.0	0.040	−1.649	−0.715
1.0	∞	−0.539	N/A
1.586	0.105	−0.757	−0.218
2.0	0.086	−0.825	−0.286
3.0	0.070	−0.831	−0.292
4.0	0.061	−0.885	−0.346

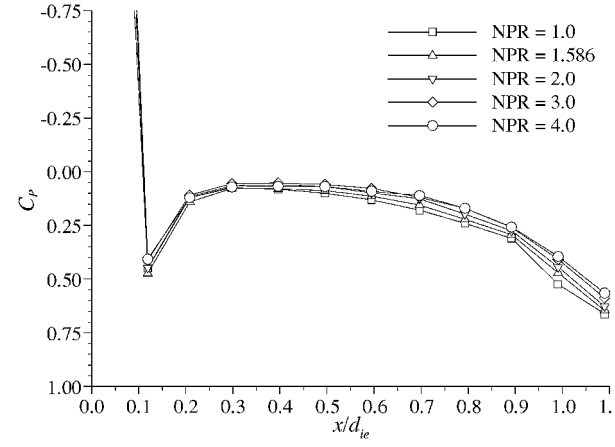

Fig. 15 Intake upper outer surface pressure distribution, intakes powered, forward nozzle position, q_∞ = 551 Pa.

the order of $-0.25C_p$. The lower pressure coefficients were caused by a combination of the action of the jet entraining ambient air, increasing the local air velocity over the intake lower surface, and a change in the local flow direction. Increasing jet to intake mass flow ratio increased the interference effect observed.

On the lower and upper intake surfaces, the main effect of the jet was to change the suction pressures around the intake lip, reducing them on the lower inner surface and increasing them on the upper inner surface.

On the upper outer surface of the intake (Fig. 15), there was a small jet-induced interference. The effect of the jet was to decrease the positive pressures on the surface of the intake. The higher the nozzle mass flow rate, the greater the jet-induced interference. The interference effect was much smaller than for the lower outer surface due to the greater distance between the upper surface of the intake and the jet. The data agree quite well with those of Mineck and Margason.[5]

The pressure distributions were integrated to give an intake normal force coefficient C_{ni} (negative indicating a downward force). This provided an indication of the changes in airload seen by the intake due to jet operation. Table 4 summarizes the variation in C_{ni} with jet operation for the center nozzle position.

Figure 16 shows the variation in C_{ni} with NPR for the three nozzle positions and a freestream dynamic pressure of 245 Pa. Increasing jet to intake mass flow ratio increased the downward force on the intake. This is due to the higher downwash velocity, which has been shown to exist in the flowfield.

Jet/Intake Mutual Interference

To determine the overall performance of the aircraft with both the jet and intakes operational, the usual practice is to take the linear

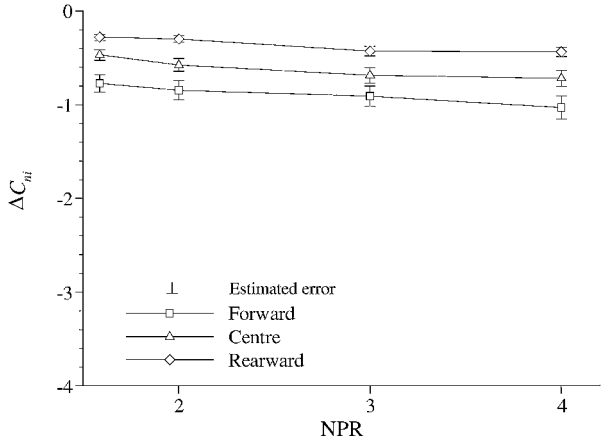

Fig. 16 Variation in C_{ni} with NPR for three nozzle positions, q_∞ = 245 Pa.

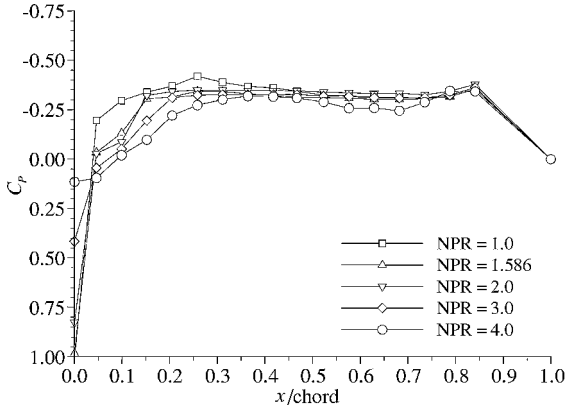

Fig. 17 Wing upper surface pressure distribution, intakes powered, forward nozzle position, q_∞ = 61.3 Pa.

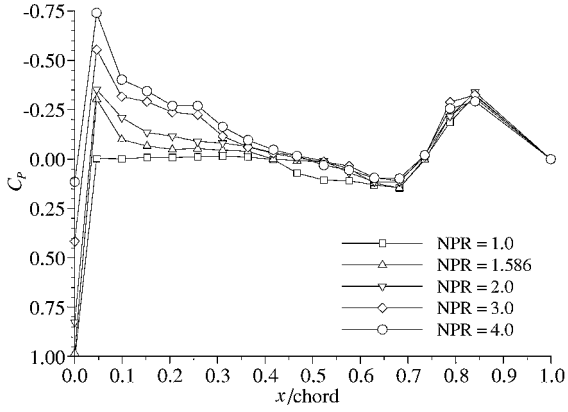

Fig. 18 Wing lower surface pressure distribution, intakes powered, forward nozzle position, q_∞ = 61.3 Pa.

sum of the jet-induced interference and intake-induced interference on the wing.

With both the jet blowing and the intakes powered, the expectation might be that the wing upper and lower surface pressure distributions would be some combination of the isolated jet and intake configurations (tests B and C) described earlier, and this was indeed the case. In general, the wing showed less negative C_p values on the upper (Fig. 17) and lower (Fig. 18) surfaces of the wing than with just the jet blowing.

Analysis of the data from simultaneous jet/intake testing shows that the numerical sum of the interference effects on the $C_{l(\text{root})}$ values generated by the jet and intake tested separately was not

Table 5 Comparison of testing jet and intakes separately and simultaneously, center nozzle position

NPR	V_e	$\Delta C_{l(\text{root})}$ (separate)	$\Delta C_{l(\text{root})}$ (together)	$\Delta C_{l(\text{root})}$ (% difference)
1.586	0.035	−0.021	−0.067	−17.68
2.0	0.029	−0.057	−0.054	1.00
3.0	0.023	−0.109	−0.178	−26.50
4.0	0.020	−0.160	−0.242	−31.55
1.586	0.070	−0.038	−0.053	−5.79
2.0	0.057	−0.057	−0.066	−3.81
3.0	0.047	−0.056	−0.071	−6.05
4.0	0.040	−0.058	−0.064	−2.53
1.586	0.105	−0.033	−0.048	−6.28
2.0	0.086	−0.048	−0.062	−5.83
3.0	0.070	−0.060	−0.072	−4.96
4.0	0.061	−0.072	−0.081	−3.85

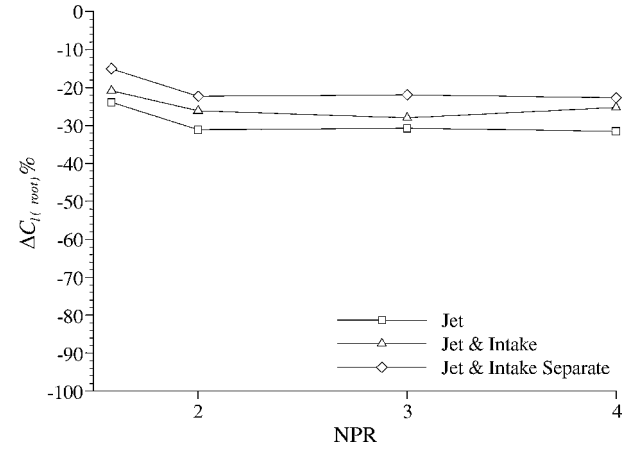

Fig. 19 Effect of separate jet and intake testing on $\Delta C_{l(\text{root})}$, center nozzle position, q_∞ = 245 Pa.

the same as with the jet and intakes in operation together. The discrepancy was the jet/intake mutual interference, in particular the effect of the jet on the intake flow. It has already been demonstrated that this is the case for constant jet/intake mass flow ratios.[7]

Figure 19 shows the effect of varying jet/intake mass flow ratio with a freestream dynamic pressure of 245 Pa and a center nozzle position. As mass flow ratio is increased, the lift loss on the wing (jet-only cases) increases. This has already been described. The combined effect of separate jet and intake testing is to shift the wing root interference lift loss, caused by the jet, a fixed amount, which was determined by the configuration C tests. This method of determining the wing lift loss only takes into account the effect of freestream dynamic pressure on the results and not the effect of NPR or nozzle position.

With the jet and intakes operating simultaneously, the wing lift loss falls between the two and follows the same NPR trend as the effect of the jet on the wing, and so, whether taken separately or together, the trend with NPR is generally the same.

Table 5 compares the $\Delta C_{l(\text{root})}$ values for separate and simultaneous jet and intake testing. It is clear that for this particular STOVL configuration the simultaneous jet and intake testing gave consistently more wing root lift loss than is obtained from separate jet and intake testing. Increasing jet/intake mass flow ratio increased the $\Delta C_{l(\text{root})}$ values for both the separate and simultaneous testing, and so this parameter does not appear to influence the magnitude of the error obtained from separate jet and intake testing, which was up to $-0.08\Delta C_{l(\text{root})}$ (0.75 deg incidence).

Conclusions

In general, the jet entrainment appeared to introduce a localized velocity component into the crossflow that altered the wing

upper and lower surface pressure distributions. The jet-induced lift loss varied between $-0.042C_{l(\text{root})}$ and $-0.234C_{l(\text{root})}$. The latter is equivalent to a reduction in wing root incidence of over 3.5 deg. The changes were found to be strongly influenced by nozzle mass flow rate and effective velocity ratio V_e.

The effect of the intakes on the wing was to create a lift enhancement. This was due to the intake flow altering the local velocity and direction of the freestream ahead of the wing. At the lowest freestream dynamic pressure tested (61.3 Pa), the lift enhancement was equivalent to a 0.5 deg increase in wing incidence. As freestream dynamic pressure was increased, the lift enhancing effect reduced becoming 0.2 deg at 245 Pa and 0.1 deg at 551 Pa.

Jet-induced interference introduced a velocity component into the freestream, which affected the intake flow as well as the airflow over the wing. This created a download on the intakes, which was determined from the intake static pressure distributions. Increasing jet/intake mass flow ratio increased ΔC_{ni}, particularly at the lowest freestream dynamic pressure.

In general, there was a discrepancy between the $\Delta C_{l(\text{root})}$ values obtained from separate and simultaneous jet and intake testing. The discrepancy between the two methods varied between -0.08 and $0.0\Delta C_{l(\text{root})}$ depending on the model configuration and test parameters. This is equivalent to nearly 0.75 deg in wing root incidence.

Acknowledgments

This research was carried out under the Engineering Doctorate scheme run by Cranfield University, and was jointly funded by the Engineering and Physical Sciences Research Council and the Defence Evaluation and Research Agency (DERA), Farnborough. The authors would like to acknowledge the assistance of R. Bruce of DERA Farnborough during this research program.

References

[1] Margason, R. J., "Fifty Years of Jet in Cross-Flow Research," *Proceedings of the 72nd AGARD Fluid Dynamics Panel Meeting and Symposium on Computational and Experimental Assessment of Jets in Cross Flow*, CP-534, April 1993, pp. 1-1–1-41.

[2] Harris, A. E., Wilde, G. L., Smith, V. J., Mundell, A. R. G., and Davidson, D. P., "ASTOVL Model Engine Simulators for Wind Tunnel Research," CP-498, AGARD Fluid Dynamics Panel Symposium, Oct. 1991, pp. 15.1–15.10.

[3] Kuhn, R. E., and McKinney, M. O., Jr., "NASA Research on the Aerodynamics of Jet VTOL Installations," AGARDograph 103, Specialists Meeting, Oct. 1965, pp. 689–713.

[4] MacLean, R., Sullivan, J., and Murthy, S. N. B., "Hot Gas Environment Around STOVL Aircraft in Ground Proximity—Part I: Experimental Study," AIAA Paper 90-2269, July 1990.

[5] Mineck, R. E., and Margason, R. J., "Pressure Distribution on a Vectored Thrust V/STOL Fighter in the Transition-Speed Range," NASA TM X-2867, 1973.

[6] Mineck, R. E., and Schwendemann, M. F., "Aerodynamic Characteristics of a Vectored Thrust V/STOL Fighter in the Transition-Speed Range," NASA TN D-7191, 1973.

[7] Saddington, A. J., and Knowles, K., "Mutual Interference Between Jets and Intakes in STOVL Aircraft," *RAeS Aeronautical Journal*, Vol. 103, No. 1024, 1999, pp. 281–286.

[8] Bray, D., "Jets in Cross-Flow and Ground Effect," Ph.D. Dissertation, Cranfield Inst. of Technology, Royal Military College of Science, Shrivenham, U.K., 1992.

[9] Kuenstner, R., Deutenbach, K., and Vagt, J., "Measurement of Reference Dynamic Pressure in Open-Jet Automotive Wind Tunnels," Society of Automotive Engineers, SAE Rept. 920344, Feb. 1992.

[10] Saddington, A. J., "Mutual Interference Between Jets and Intakes in STOVL Aircraft," Eng. D. Dissertation, Cranfield Univ., Royal Military College of Science, Shrivenham, U.K., 1997.

[11] "Lift-Curve Slope and Aerodynamic Centre Position of Wings in Inviscid Subsonic Flow," Data Item 70011, ESDU International plc, London, 1993.